CrystEngComm

PAPER

View Article Online
View Journal | View Issue

Cite this: *CrystEngComm*, 2019, **21**, 236

Unique crystallographic signatures of Boc-Gly-Phe-Phe-OMe and Boc-Gly-Phg-Phe-OMe and their self-association†

Rajat Subhra Giri and Bhubaneswar Mandal *

The self-assembly of N- and C-protected tripeptides, Boc-Gly-Phe-Phe-OMe (**1**) and its analog Boc-Gly-Phg-Phe-OMe (**2**, Phg = phenylglycine), has been investigated. The presence of just an extra methylene ($-CH_2-$) group in the side chain of one of the amino acids resulted in significant changes in their molecular arrangement and supramolecular structure. The single crystal X-ray diffraction analysis suggested that **1** adopted a type II β-turn-like conformation, known as open turn identified by the absence of any intramolecular hydrogen bond, which further self-assembled to form a herringbone helix-like architecture through non-covalent interactions. To the best of our knowledge, this is the first report on a designed open turn tripeptide without a kink-forming element. However, in spite of the presence of a non-standard amino acid **2** adopted a β-sheet conformation which further self-organized to form a helical architecture through non-covalent interactions in the crystalline form. The conformations of these peptides in solution were also investigated by solvent dependent NMR titration, 2D NOESY, and CD spectroscopic experiments. These peptides exhibited two different flower-like architectures in acetonitrile–water medium under an optical microscope and a field emission scanning electron microscope (FESEM).

Received 10th October 2018,
Accepted 20th November 2018

DOI: 10.1039/c8ce01723a

rsc.li/crystengcomm

Introduction

The self-assembly of small di- or tripeptides to form various micro- or nanoscale structures has essential applications in bioorganic chemistry, materials science, nanotechnology, and medicinal chemistry.[1–4] Helical structures, *e.g.*, α-helix of protein,[5] single stranded helical RNA,[6] double stranded helix of DNA[7] and triple-stranded collagen helix,[8] play essential roles in biological systems. Moreover, like β-sheet structures, helical structures also have an essential role in the formation of self-aggregated amyloid fibrils.[9] Therefore the development of *de novo* designed helical assembly is essential.

Banerjee *et al.* reported that unnatural amino acids, such as Aib (α-aminoisobutyric acid), containing tripeptides form a supramolecular helical assembly where no intramolecular H-bond is present.[10] They also reported the double helical structure of dipeptides and single stranded helical assembly of tetrapeptides that contain a β-alanine residue at the N-terminus.[11,12] Görbitz described the double helical structures of a dipeptide belonging to the Val-Ala class.[13] Haldar and co-workers reported that N-terminal L-tyrosine and central Aib containing tripeptides form a supramolecular double helix from distorted type II or type II' or water-mediated type II β-turn in higher order assembly in the solid state.[14] They also reported the helical structure of a dipeptide containing N-terminal L-phenylalanine and C-terminal rigid aromatic β/γ/δ amino acids.[15] Sanjayan *et al.* reported the left and right-handed helical structures of carboxamide and sulfonamide of $(Pro\text{-}Ant\text{-}Aib)_n$ oligomers, respectively.[16] Huc and co-workers discussed the construction of a herringbone helix from aromatic–aliphatic δ-peptides.[17] Balaram *et al.* reported that α,α-di-*n*-propylglycine (Dpg) and α,α-di-*n*-butylglycine (Dbg) containing tripeptides adopted a distorted type II β-turn devoid of intramolecular H-bonds known as the open turn.[18,19] These peptides had a tendency to form a helix. Pramanik *et al.* described a similar open turn[20] formation by *m*-aminobenzoic acid and Aib containing tripeptides. They also reported the interconversion between the β-turn or hydrated β-turn and β-strand of tripeptides which contain an Aib amino acid residue as a central position of its sequence.[21]

Herein, we present the self-assembly, conformation, and morphology of both N- and C-protected tripeptides Boc-Gly-Phe-Phe-OMe (**1**) and its analog Boc-Gly-Phg-Phe-OMe (**2**, Fig. 1).

Department of Chemistry, Laboratory of Peptide and Amyloid Research, Indian Institute of Technology Guwahati, Assam- 781039, India.
E-mail: bmandal@iitg.ernet.in

† Electronic supplementary information (ESI) available: 2D NMR, titration data and plot, crystallographic data, Hirshfeld data, HPLC profiles, and characterization spectra of all the synthesized peptides. CCDC 1851441 and 1851442. For ESI and crystallographic data in CIF or other electronic format see DOI: 10.1039/c8ce01723a

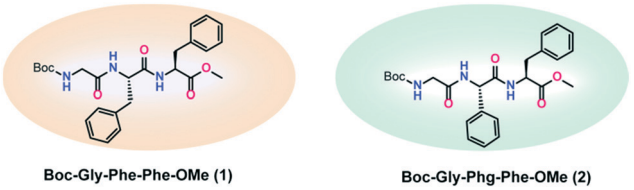

Fig. 1 The chemical structures of tripeptides **1** and **2**.

In **2**, N-terminal Phe is replaced by Phg (phenylglycine) which is a non-coded non-standard amino acid, and it has one carbon (–CH_2–) less in the side chain than that of Phe. Comparative studies were initially planned to investigate whether the more rigid side chain of Phg plays any role in inducing a turn in the peptide backbone similar to Aib and analogs. Such knowledge could be useful for β-sheet breaker peptide design for our amyloid research.[22,23]

The results are surprising and exciting. The single crystal X-ray diffraction analysis revealed that **1** formed a distorted type II β-turn known as the open turn[18,19] structure which further self- assembled to form a supramolecular herringbone helix-like architecture in a higher order. The reported examples of open turn structures are very few in the literature. The open turn structure is very similar to the type II β-turn but does not contain an intramolecular (4 → 1) hydrogen bond to form the 10-membered cyclic ring. Furthermore, most of the reported open turn[18,20,24] structures contained pre-organized kink-forming moieties. Interestingly enough, **1** produced such a type of open turn conformation without the help of any pre-organized kink forming moiety, while **2** did not deviate substantially from the parallel β-sheet arrangement despite the presence of a non-standard amino acid (Phg). It further self-assembled to form a supramolecular helical architecture. We also performed various biophysical studies, *e.g.*, circular dichroism (CD), field emission scanning electron microscopy (FESEM) and transmission electron microscopy (TEM), to understand the conformation and morphology of these peptides.

After the synthesis using conventional coupling methods in solution (Scheme 1)[25,26] the peptides were purified by column chromatography. Characterization was performed by

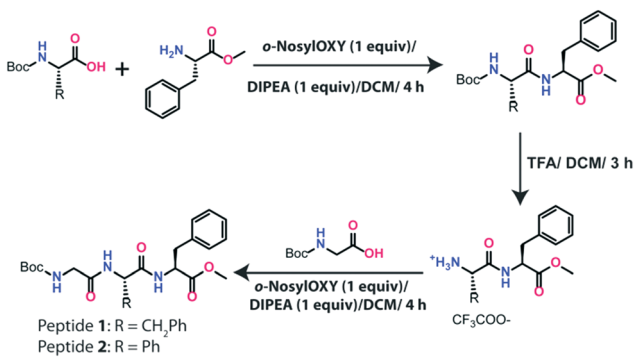

Scheme 1 Peptide synthesis using conventional coupling methods in solution.

1D [1H] and 2D [1H, 1H] NMR spectroscopy as well as mass spectrometry.

At first, we performed single crystal X-ray diffraction (SC-XRD) experiments to obtain the structural details of these peptides. Colorless block-shaped crystals of **1** and **2** were grown from acetonitrile–water medium by slow evaporation at room temperature (ESI,† Fig. S1). Both **1** and **2** exhibited a monoclinic ($P2_1$) space group in their crystalline form and also showed one molecule in the asymmetric unit. The measured backbone torsion angles ($\varphi1$ = −56.1, $\psi1$ = 145.8 and $\varphi2$ = 59.8, $\psi2$ = 29.7, Table 1) indicated that **1** adopts a conformation similar to the type II β-turn[14,21] (Fig. 2a) but slightly deviated from the ideal values ($\varphi1$ = −60, $\psi1$ = 120 and $\varphi2$ = 80, $\psi2$ = 0) of the type II β-turn.[19,27,28] Although no intramolecular H-bond between *i* (Boc-CO) and *i* + 3 (NH of Phe 2) was observed, the distance between them, *i.e.*, N3···O2 and O2···H3N hydrogen bond distances, was 3.24 and 2.58 Å, respectively, which were close to the ideal 10-membered intramolecular hydrogen bonded type II β-turn (N···O = 3.15 Å and O···HN = 2.35 Å).[29] For comparison, Boc-Ala-Aib-Ala-OMe and Ac-Ala-Aib-Ala-OMe exhibited a distorted β-turn with a 3.6 Å (N···O distance) long intramolecular 4 → 1 hydrogen bond.[30,31] Furthermore, although **1** did not contain any intramolecular H-bond between *i* and *i* + 3 the observed torsion angles (φ and ψ) of the *i* + 1 (Gly) and *i* + 2 (Phe) amino acid residues fell close to the type II β-turn region in the Ramachandran plot.[19,27,28]

Most interestingly, such distorted type II β-turns without intramolecular H-bonding are known as open turn structures and are formed by pre-organized kink inducing non-natural amino acids.[18,20,24]

The structure of **1** is unique as it forms an open turn without any turn inducing element. There are four intermolecular H-bonds, *i.e.*, two N1–H1···O3 and two N2–H2···O4, in **1** (ESI,† Table S1). One β-turn subunit of **1** is connected through N2–H2···O4 in a parallel manner and through N1–H1···O3 in an anti-parallel manner (Fig. 2b) along the *b*-axis. Next, it self-organized to form a supramolecular herringbone-like helical architecture in higher-order packing through intermolecular C–H···O interaction along the *c*-axis (Fig. 2c).

On the other hand, **2** showed a parallel β-sheet (Table 1) structure (Fig. 3a) in the solid state. The presence of Phg instead of Phe in **2** extended the backbone unlike **1**. It contained two N1–H1···O2 and two N2–H2···O3 intermolecular H-bonds (ESI,† Table S1) and each subunit of **2** is connected through those bonds to form a supramolecular β-sheet structure with a meridional distance of 4.97 Å along the *b*-axis (Fig. 3b). This also further self-assembled to form a helical structure through intermolecular C–H···O and C–H···π interactions in higher-order packing (Fig. 3c) along the crystallographic *c*-axis. The bond distance of C–H···O and C–H···π was 2.62 Å and 2.88 Å, respectively. The crystallographic data are displayed in Table 2.

Interestingly, incorporation of Phg, *i.e.*, one carbon (–CH_2–) less in the side chain than that of Phe, in **2** deviated the crystal structure from that of **1** significantly.

Table 1 The backbone torsion angles (deg) of **1** and **2**

Boc-Gly-Phe-Phe-OMe (1)	Torsion angles (deg)	Boc-Gly-Phg-Phe-OMe (2)
C5–N1–C6–C7 = −56.1(8)	$\varphi 1$	C5–N1–C6–C7 = 126.2(3)
C7–N2–C8–C16 = 59.8(7)	$\varphi 2$	C7–N2–C8–C15 = −127.6(3)
C16–N3–C17–C25 = −51.6(7)	$\varphi 3$	C15–N3–C16–C24 = −159.9(3)
N1–C6–C7–N2 = 145.8(5)	$\psi 1$	N1–C6–C7–N2 = −121.4(3)
N2–C8–C16–N3 = 29.7(8)	$\psi 2$	N2–C8–C15–N3 = 124.4(3)
N3–C17–C25–O6 = 136.4(5)	$\psi 3$	N3–C16–C24–O6 = −179.0(3)
O1–C5–N1–C6 = 175.2(5)	$\omega 1$	O1–C5–N1–C6 = −177.7(3)
C6–C7–N2–C8 = 178.1(5)	$\omega 2$	C6–C7–N2–C8 = 178.1(3)
C8–C16–N3–C17 = 172.0(5)	$\omega 3$	C8–C15–N3–C16 = −175.9(3)

Due to the presence of the phenyl ring close to Cα (C8) of **2**, a steric repulsion arises between the *ortho* protons of the phenyl ring and the Cα (C8) proton and NH of Phg (N2H) (Fig. 4). Thus, the phenyl ring gets tilted, and the bond angle of N–Cα–C (τ) is reduced to 107.8(8)° (N2–C8–C15) (Fig. 4). Therefore, the backbone was extended further, and the C═O of i (Boc) and N–H of i + 3 (Phe) were oriented in the opposite direction (Fig. 4), favoring the formation of a β-sheet structure. On the other hand, due to the presence of an extra carbon (–CH_2–) of Phe1 (Fig. 4) attached to Cα, the sp3 carbon (C8) became more flexible and therefore the backbone could arrange to a more stable orientation resulting in the open type II β-turn. The τ angle (N2–C8–C16) was 113.0(5)° and the C═O of i (Boc) and N–H of i + 3 (Phe 2) were oriented in the same direction (Fig. 4) but could not form 4 → 1 intramolecular H-bonds probably due to the high $\psi 1$ (145.8) value compared to the intramolecular H-bonded β-turns (127.5).[29]

However, both of these peptides exhibited a turn-like conformation in solution, supported by 2D NOESY interactions and CD profiles (Fig. 5 and 6, *vide infra*). The conformation of the peptides was investigated by NMR experiments in solution. A solvent titration experiment was performed to understand whether the hydrogen bonds are intra or intermolecular. This solvent titration was carried out by adding d_6-DMSO to the $CDCl_3$ solution of these peptides. Generally, d_6-DMSO acts as a hydrogen bond accepting solvent and therefore when its concentration is increased peptide NHs are shifted to the downfield region.

The results obtained from the NMR solvent titration illustrated that by increasing the concentration of d_6-DMSO in $CDCl_3$ (v/v) from 0 to 12% for **1** and 0 to 20% for **2** the deviation in chemical shift ($\Delta\delta$(NH)) increased by more than 0.2 ppm (ESI† Table S3, Fig. S7 for **1** and Table S5, Fig. S17 for **2**) indicating that NHs were involved in intermolecular hydrogen bonding.[32] Moreover, the specific NOE interactions obtained from the 2D [^{1}H, ^{1}H] NOESY experiment in $CDCl_3$ (Fig. 5 and ESI† Fig. S10 and S21) supported the formation of the turn-like structure[32] of both peptides in solution.

CD is a valuable tool to understand the conformation of a peptide or protein in solution. Peptide **1** (Fig. 6, dark cyan curve) showed positive Cotton effects at 217 and 198 nm, whereas **2** (Fig. 6, orange curve) exhibited positive Cotton effects at 215

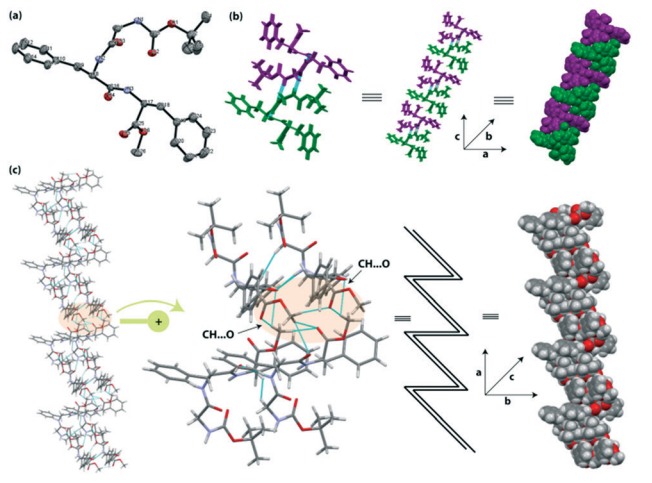

Fig. 2 (a) The ORTEP diagram with ellipsoid of 30% probability, (b) intermolecular H-bonding structure along the *b*-axis and (c) herringbone helical architecture in higher order assembly along the *c*-axis of peptide **1**.

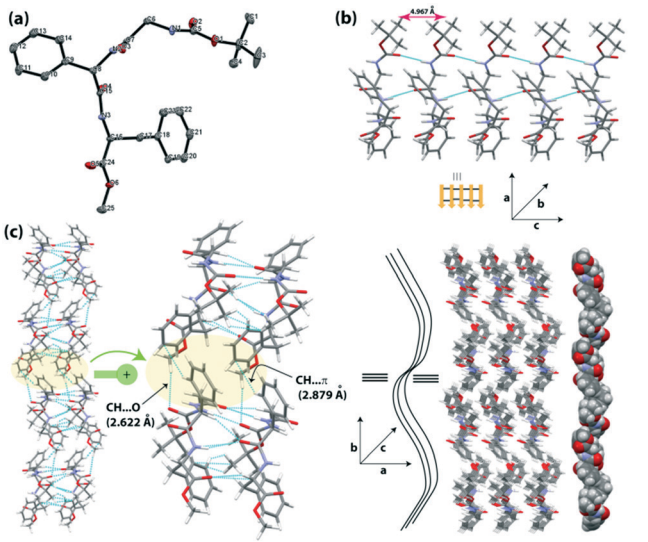

Fig. 3 (a) The ORTEP diagram with ellipsoid of 30% probability, (b) parallel β-sheet along the *b*-axis, and (c) helical arrangement in higher order assembly along the *c*-axis of **2**.

Table 2 Crystal parameters and refinement data of **1** and **2**

Parameters	Boc-Gly-Phe-Phe-OMe (1)	Boc-Gly-Phg-Phe-OMe (2)
Formula	$C_{26}H_{33}N_3O_6$	$C_{25}H_{31}N_3O_6$
Fw	483.55	469.53
Crystal system	Monoclinic	Monoclinic
Space group	$P2_1$	$P2_1$
a/Å	15.407(2)	4.96731(12)
b/Å	5.8843(6)	19.4022(5)
c/Å	15.664(2)	12.4703(3)
α/°	90.00	90.00
β/°	114.753(18)	92.486(3)
γ/°	90.00	90.00
V/Å^3	1289.6(3)	1200.72(5)
Z	2	2
D_c/g cm^{-3}	1.245	1.299
μ Mo K$_\alpha$/mm^{-1}	0.089	0.093
F000	516.0	500.0
T/K	293(2)	149.99(10)
θ max.	28.746	24.996
Total no. of reflections	6575	3488
Independent reflections	4934	2716
Observed reflections	3405	2545
Parameters refined	321	311
R_1, $I > 2\sigma(I)$	0.0721	0.0346
wR_2, $I > 2\sigma(I)$	0.1949	0.0996
GOF (F^2)	1.029	0.608
CCDC no.	1851441	1851442

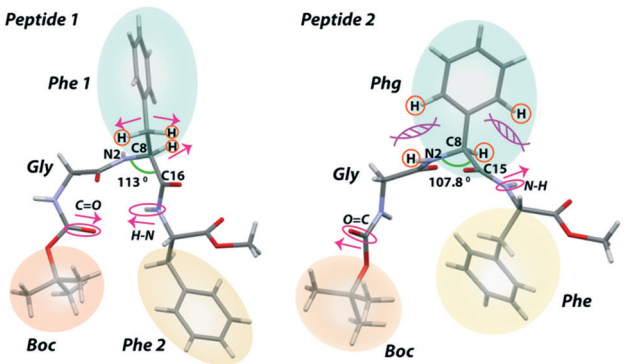

Fig. 4 Comparison of the molecular structures of **1** and **2**.

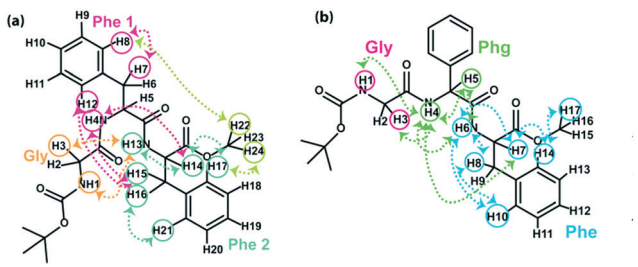

Fig. 5 Various characteristic NOEs of (a) **1** and (b) **2**, obtained from 2D NOESY.

and 202 nm indicating that both peptides contained a mixture of β-turn and β-sheet structure after seven days of incubation in 30% acetonitrile–water medium.[21]

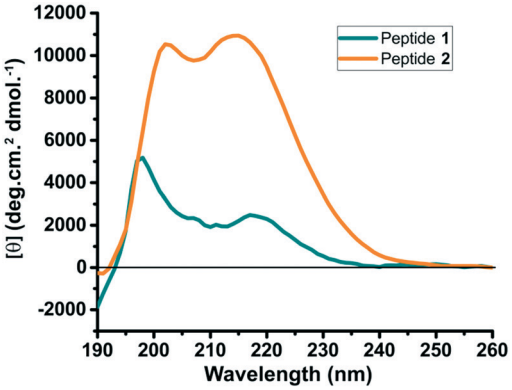

Fig. 6 CD spectra of **1** (dark cyan curve) and **2** (orange curve).

Pramanik and co-workers noted that Boc-Ile-Aib-Phe-OMe adopted a β-strand structure in the solid state, but it exhibited a mixture of hydrated β-turn and β-strand conformations in solution as suggested by the CD experiment.[21] In our case, the CD profile of **1** and **2** was similar to that of Boc-Ile-Aib-Phe-OMe suggesting the co-existence of β-turn and β-strand conformations. This indicates that although **1** and **2** adopted an open turn and β-sheet structure in the solid state, respectively, probably their conformations changed partially in solution.

Then we checked the morphology of these peptides to understand their self-association behavior. The morphologies of these self-aggregated tripeptides were analyzed under an optical microscope, a FESEM and a TEM. For this purpose, we prepared 1.5 mM solution of each of them in 30% acetonitrile–water and incubated them at 37 °C for seven days. These solutions were drop-cast on a microscopic slide for analysis using an optical microscope and over Al-foil for the FESEM study. The obtained optical images indicated that both of these peptides self-aggregated to form two different flower-like structures (Fig. 7, 1a and 2a and ESI† Fig. S2).

Similarly, the obtained FESEM images of **1** and **2** indicated that they self-aggregated to form highly organized two

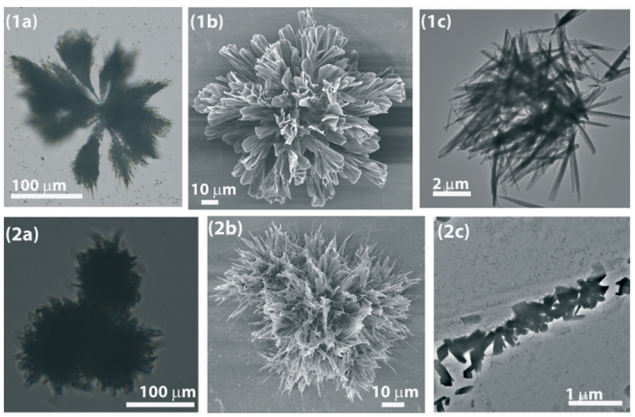

Fig. 7 Optical microscopic, FESEM and TEM images of self-aggregated tripeptides (1a), (1b) and (1c) of **1** and (2a), (2b) and (2c) of **2**, respectively, in 30% acetonitrile–water medium using a concentration of 1.5 mM.

different flower-like structures (Fig. 7, 1b and 2b and ESI† Fig. S2) in 30% CH_3CN–H_2O solution.

Next, to get a detailed morphological insight into these self-associated peptides, TEM experiments were performed. While **1** exhibited a needle-like structure under TEM, **2** organized in block-shaped structures (Fig. 7, 1c and 2c and ESI† Fig. S2). These needle and block-shaped flakes observed under TEM self-assembled to form different flower-like morphologies viewed under FESEM.

Then, we checked their Hirshfeld surfaces (HSs)[33] and 2D fingerprint plots (FPs)[34] using the Crystal Explorer program to understand the intermolecular interactions present among the molecules. In the HS map, the presence of red regions indicated the existence of intermolecular H-bonds (O···H–N/N–H···O).[35] This experiment also supported the existence of the intermolecular H-bonds found in the single crystal XRD structures (Fig. 8). Moreover, the 2D FPs denoted the distance from HSs to d_i (interior of the surface) and d_e (exterior of the surface). The spikes produced in the 2D FPs suggested that the position of interaction existed in the HSs. Here, 20% and 23.4% O (interior atom)···H (exterior atom) interactions of **1** and **2** were obtained from the 2D FPs, respectively (Fig. 8 and Table S6†).

Experimental

General information

All Boc protected amino acids, Oxyma and 2-nitrobenzenesulfonyl chloride were obtained from GL Biochem (Shanghai). *N*,*N*-Diisopropylethylamine (DIPEA), dichloromethane (extra pure grade), acetonitrile (HPLC grade) and trifluoroacetic acid (TFA) were purchased from Spectrochem (India). Citric acid, sodium bicarbonate ($NaHCO_3$) and DMSO-d_6 were obtained from Merck (India). $CDCl_3$ was purchased from Sigma Aldrich.

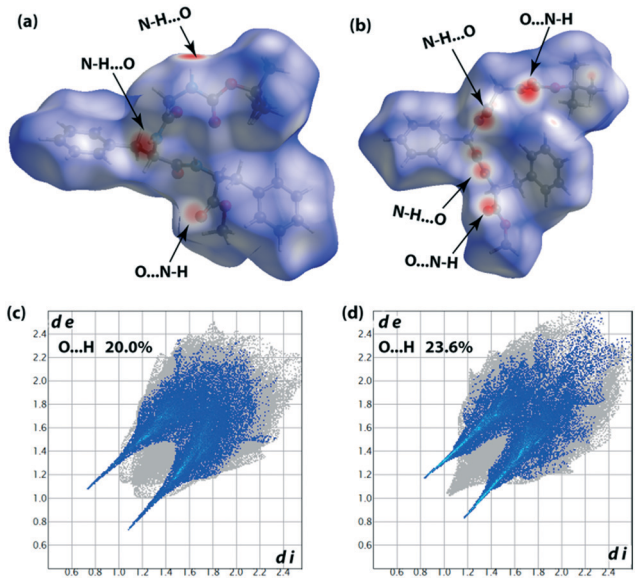

Fig. 8 Hirshfeld surface map of (a) **1** and (b) **2**. 2D fingerprint plots for (c) **1** and (d) **2** with O···H interactions.

Peptide synthesis

The N-terminal *t*-butyloxycarbonyl (Boc) protected amino acid (1 equiv.), coupling reagent, *o*-NosylOXY (1 equiv.), Hünig's base DIPEA (1 equiv.) in dichloromethane (DCM) were taken in a 50 mL round-bottom flask (RB) and the mixture was kept for 5 min for preactivation.[25] In another beaker, the methyl ester of the next amino acid (1.2 equiv.) with DIPEA (1.2 equiv.) in DCM was taken for neutralization. Then, this solution was added dropwise to the above reaction vessel and kept stirring for 4–5 h at room temperature. After completion of the reaction, the reaction mixture was diluted with DCM and washed with a 10% citric acid solution followed by the saturated $NaHCO_3$ solution 3 times, in each case. Then, the organic layer was dried over anhydrous Na_2SO_4, and the decanted solvent was evaporated to get the solid N- and C-protected dipeptide. Next, this dipeptide was taken in a 50 mL RB and TFA : DCM (90 : 10) was added into it. After 3 h of reaction, the TFA was evaporated by passing N_2 over the solution which was again neutralized by adding DIPEA. Then this Boc deprotected dipeptide was coupled with the next Boc-*N*-amino acid, using the procedure mentioned earlier to get the tripeptide. The desired product was purified by silica gel column chromatography using an ethyl acetate–hexane solvent system.

Synthesis of peptide 1

At first, 500 mg (1.886 mmol) of Boc-Phe-OH was dissolved in 10 mL DCM and then 617 mg (1.886 mmol) of *o*-NosylOXY and 243 mg (1.886 mmol) of DIPEA were added to the solution which was kept stirring for 5 min for preactivation. After that, 405 mg (2.263 mmol) of H-Phe-OMe was neutralized by 292 mg (2.263 mmol) of DIPEA which was added to the above reaction vessel and stirred for 4 h at room temperature. After completion of the reaction, the reaction mixture was worked up and the obtained solid dipeptide, Boc-Phe-Phe-OMe, was treated with TFA to remove the Boc protecting group. Then, the amine free H-Phe-Phe-OMe was coupled with Boc-Gly-OH within 4 h. After purification by column chromatography, we obtained a white solid of Boc-Gly-Phe-Phe-OMe (**1**). The purity of the peptides was confirmed using analytical HPLC. The isolated peptides were characterized by mass spectrometry as well as 1D [^{1}H] (^{1}H and ^{13}C) and 2D (COSY, TOCSY, HSQC, NOESY) NMR spectroscopy (Fig. S3–S12†).

White solid, mp 158–160 °C, ^{1}H NMR ($CDCl_3$; 600 MHz) δ 1.44 (9H, s); 3.08–2.95 (4H, m); 3.67 (3H, s); 3.77–3.69 (2H, m); 4.68–4.65 (1H, q, J = 7.2 Hz, J = 7.2 Hz); 4.77–4.74 (1H, q, J = 6.6 Hz, J = 7.2 Hz); 5.13 (1H, brs); 6.48 (1H, brs); 6.74–6.73 (1H, d, J = 7.8 Hz), 7.01–7.00 (2H, d, J = 6.6 Hz); 7.16–7.15 (2H, d, J = 6.6 Hz), 7.26–7.20 (6H, m). ^{13}C NMR ($CDCl_3$; 150 MHz) δ 28.4, 37.9, 44.3, 52.5, 53.5, 54.2, 80.5, 127.2, 127.3, 128.7, 128.8, 129.3, 135.8, 136.3, 156.1, 169.5, 170.4, 171.5. HRMS (ESI): calculated $[M + H]^+$ 484.2369, found *m*/*z*.

484.2529. HPLC: retention time (t_R) = 8.90 min. Isolated pure product 663 mg (yield: 73% w.r.t. starting material Boc-Phe).

Synthesis of peptide 2

At first, 500 mg (1.992 mmol) of Boc-Phg-OH was dissolved in 10 mL DCM, and then 651 mg (1.992 mmol) of *o*-NosylOXY and 257 mg (1.992 mmol) of DIPEA were added to the solution which was kept stirring for 5 min for preactivation. After that, 428 mg (2.390 mmol) of H-Phe-OMe was neutralized by 308 mg (2.390 mmol) of DIPEA which was added to the above reaction vessel and stirred for 4 h at room temperature. After completion of the reaction, the reaction mixture was worked up and the obtained solid dipeptide, Boc-Phg-Phe-OMe, was treated with TFA to remove the Boc protecting group. Then, the free amine of H-Phg-Phe-OMe was coupled with Boc-Gly-OH for 4 h. After purification by column chromatography, we obtained a white solid of Boc-Gly-Phg-Phe-OMe (**2**). The purity of the peptides was confirmed using analytical HPLC. The isolated peptides were characterized by mass spectrometry as well as 1D [^{1}H] (^{1}H and ^{13}C) and 2D (COSY, TOCSY, HSQC, NOESY) NMR spectroscopy (Fig. S13–S22†).

White solid, mp 157–159 °C, ^{1}H NMR ($CDCl_3$; 600 MHz) δ 1.43 (9H, s); 3.07–3.03 (1H, dd, J = 6 Hz); 3.17–3.13 (1H, dd, J = 5.4 Hz); 3.64 (3H, s); 3.86–3.76 (2H, m); 4.81–4.78 (1H, q, J = 6 Hz, J = 7.8 Hz); 5.21 (1H, brs); 5.47–5.46 (1H, d, J = 6.6 Hz); 6.47 (1H, brs), 7.07–7.06 (2H, d, J = 7.2 Hz); 7.29–7.23 (8H, m). ^{13}C NMR ($CDCl_3$; 150 MHz) δ 28.4, 37.8, 44.3, 52.5, 53.7, 57.2, 80.4, 127.4, 127.5, 128.7, 128.8, 129.2, 129.4, 135.7, 137.0, 156.2, 169.1, 169.5, 171.5. HRMS (ESI): calculated $[M + H]^+$ 470.2213, found m/z. 470.2298. HPLC: retention time (t_R) = 8.74 min. Isolated pure product 668 mg (yield: 71% w.r.t. starting material Boc-Phg).

High-performance liquid chromatography (HPLC)

The purity of these peptides was checked with an analytical HPLC, Thermo Scientific Dionex Ulti Mate 3000 Rapid Separation LC (RSLC) system, using a C18 Thermo Scientific column at a flow rate of 1 mL min^{-1}, with a linear gradient of 5–100% CH_3CN over 8 minutes in a total run time of 20 min. A binary solvent system, solvent A (H_2O) and solvent B (CH_3CN), was used. A dual wavelength UV detector (at 214 and 254 nm) was used.

Mass spectrometry

The mass spectra of the peptide samples were obtained from an Agilent-Q-TOF 6500 instrument. All data were collected in ESI positive mode and analyzed with Mass hunter workstation software.

Nuclear magnetic resonance (NMR) spectroscopy

All NMR spectra were recorded on a Bruker Ascend 600 MHz instrument at 298 K using $CDCl_3$ solvent. 1D [^{1}H] spectra and 2D [^{1}H, ^{1}H] TOCSY (total correlation spectroscopy), 2D [^{1}H, ^{1}H] COSY (correlated spectroscopy), and 2D [^{1}H, ^{13}C] HSQC (heteronuclear single quantum coherence) were recorded with NS = 16 scans and 2D [^{1}H, ^{1}H] NOESY (nuclear Overhauser enhancement spectroscopy) was recorded with NS = 32 scans. Chemical shifts were referenced to $CDCl_3$ at δ = 7.26 ppm and δ = 77.23 in ^{1}H NMR and ^{13}C NMR, respectively.

Single crystal X-ray diffraction (SC-XRD)

The single crystal XRD experiment was carried out using an Oxford SuperNova diffractometer. Data collection was carried out by SMART software. Data refinement and cell reductions were performed by CrysAlisPro.[36] The obtained structures were solved by direct methods. The refinement was performed by SHELXTL software[37] using full-matrix least-squares calculations.

Sample preparation

2.07 mM peptide **1** and 2.13 mM peptide **2** solutions were prepared in two different Eppendorf vials (2 mL) by adding 1 mL 30% $CH_3CN:H_2O$ solution. Then, we prepared a 1 mL (1.5 mM) solution (stock solution) from the above solutions for each peptide. These stock solutions were incubated for 7 days at 37 °C. After 7 days, we prepared IR, FESEM, TEM, and microscopic slid samples.

Circular dichroism (CD)

CD spectra were obtained from a JASCO J-1500 instrument. After 7 days, 400 μL of each solution was taken in a CD cuvette, and CD spectra were recorded from 190 nm to 260 nm wavelength using 1 mm path length and 1 nm bandwidth. The mean residue molar ellipticity was calculated using the following equation:

$$\theta(\text{deg cm}^2\ \text{dmol}^{-1}) = \text{Ellipticity (mdeg)}\cdot 10^6/\text{Pathlength (mm)}\cdot[\text{Protein}](\mu\text{M})\cdot N$$

Optical microscopic images

10 μL of 7 day old samples were drop cast on the microscopic slide and dried. The bright field images (40× magnificence) were recorded on a Nikon Digital Sight DS-U3 microscope.

Field emission scanning electron microscopy (FESEM)

FESEM samples were made by drop casting (10 μL) 1.5 mM peptide **1** and peptide **2** on Al-foil and dried overnight inside a desiccator. FESEM images were captured using a SIGMA-300 (ZEISS) instrument.

Transmission electron microscope (TEM)

After 7 days of incubation at 37 °C, the 1.5 mM concentration was converted to 100 μM and from this 10 μL of each sample was drop-casted on a carbon-coated copper grid, followed by adding 2% uranyl acetate solution (10 μL), and allowed to float for 1 min. After removing the excess solution by blotting

paper, the samples were kept inside a desiccator. TEM images were recorded under a JEOL (Model: 2100F) instrument.

Hirshfeld surface analysis

Hirshfeld surfaces and 2D fingerprint plots were recorded using the Crystal Explorer 3.1 program.[38]

Conclusions

In conclusion, we investigated the crystallographic signatures of the self-assembled supramolecular helical architectures of Boc-Gly-Phe-Phe-OMe (**1**) and Boc-Gly-Phg-Phe-OMe (**2**). SC-XRD revealed that **1** formed a distorted type II β-turn conformation, called the open turn, which further self-assembled through intermolecular C–H···O bonding to form a herringbone helical architecture along the crystallographic *c*-axis. Such open turn formation is unusual for a standard amino acid containing the designed tripeptide without a kink-forming element like proline or Aib. Alternatively, **2** exhibited a β-sheet structure which further self-assembled through intermolecular C–H···O and C–H···π bonding to form a helical architecture along the *c*-axis in the solid state. However, in solution, both **1** and **2** exhibited a mixture of β-turn and β-strand structures, supported by NMR and CD experiments. Further, they self-associated to form two different flower-like architectures in 30% acetonitrile–water medium. The differences in molecular and supramolecular level structural arrangements of these two peptides are due to the presence of the methylene group at the side chain of only one amino acid (Phe), which is the only difference in their chemical structures. This work may open up an avenue for the design of open turn structures without using any pre-organized kink inducing moieties. Formation of such a type of assembly may be useful for designing nanostructures for nanotechnology and materials chemistry. Furthermore, as **1** contain C-terminal phenylalanylphenylalanine (–Phe-Phe–) residues, identical with the core hydrophobic self-recognizing unit of the amyloid-β peptide, such structural insight may be useful for amyloid research.

Conflicts of interest

There are no conflicts of interest to declare.

Acknowledgements

We are thankful to Central Instruments Facility (CIF) for single-crystal XRD, FESEM and NMR facilities, the Department of Chemistry, Indian Institute of Technology, Guwahati for other instrumental facilities and SC-XRD facility, AMRC at IIT Mandi and the Department of Biotechnology, Govt. of India, for financial support (twinning program for the North Eastern Region, sanction no. BT/PR16164/NER/95/88/2015). We are also thankful to Mr. Utsab Manna for crystal analysis.

Notes and references

1 I. P. Moreira, T. K. Piskorz, J. H. Van Esch, T. Tuttle and R. V. Ulijn, *Langmuir*, 2017, **33**, 4986–4995.
2 Y. Li, Y. Wang, G. Huang and J. Gao, *Chem. Rev.*, 2018, **118**, 5359–5391.
3 D. Mandal, A. Nasrolahi Shirazi and K. Parang, *Org. Biomol. Chem.*, 2014, **12**, 3544–3561.
4 N. Habibi, N. Kamaly, A. Memic and H. Shafiee, *Nano Today*, 2016, **11**, 41–60.
5 D. Sali, M. Bycroft and A. R. Fersht, *Nature*, 1988, **335**, 740–743.
6 C. D. Eichhorn and H. M. Al-Hashimi, *RNA*, 2014, **20**, 782–791.
7 P. Wittung, P. E. Nielsen, O. Buchardt, M. Egholm and B. Nordén, *Nature*, 1994, **368**, 561–563.
8 D. R. Eyre, *Science*, 1980, **207**, 1315–1322.
9 C. Goldsbury, K. Goldie, J. Pellaud, J. Seelig, P. Frey, S. A. Müller, J. Kistler, G. J. S. Cooper and U. Aebi, *J. Struct. Biol.*, 2000, **130**, 352–362.
10 D. Haldar, S. K. Maji, W. S. Sheldrick and A. Banerjee, *Tetrahedron Lett.*, 2002, **43**, 2653–2656.
11 S. Guha, M. G. B. Drew and A. Banerjee, *Org. Lett.*, 2007, **9**, 1347–1350.
12 A. Banerjee, S. K. Maji, M. G. B. Drew, D. Haldar and A. Banerjee, *Tetrahedron Lett.*, 2003, **44**, 699–702.
13 C. H. Görbitz, *Chem. – Eur. J.*, 2007, **13**, 1022–1031.
14 P. Jana, S. Maity, S. K. Maity and D. Haldar, *Chem. Commun.*, 2011, **47**, 2092–2094.
15 S. Maity, P. Jana, S. K. Maity, P. Kumar and D. Haldar, *Cryst. Growth Des.*, 2012, **12**, 422–428.
16 V. V. E. Ramesh, S. S. Kale, A. S. Kotmale, R. L. Gawade, V. G. Puranik, P. R. Rajamohanan and G. J. Sanjayan, *Org. Lett.*, 2013, **15**, 1504–1507.
17 H. Jiang, J. M. Leger and I. Huc, *J. Am. Chem. Soc.*, 2003, **125**, 3448–3449.
18 M. Crisma, G. Valle, C. Toniolo, S. Prasad, R. Balaji Rao and P. Balaram, *Biopolymers*, 1995, **35**, 1–9.
19 G. D. Rose, L. M. Gierasch and J. A. Smith, *Adv. Protein Chem.*, 1985, **37**, 1–109.
20 A. Dutt, M. G. B. Drew and A. Pramanik, *Tetrahedron*, 2005, **61**, 11163–11167.
21 A. Dutt, A. Dutta, R. Mondal, E. C. Spencer, J. A. K. Howard and A. Pramanik, *Tetrahedron*, 2007, **63**, 10282–10289.
22 A. Paul, K. C. Nadimpally, T. Mondal, K. Thalluri and B. Mandal, *Chem. Commun.*, 2015, **51**, 2245–2248.
23 A. Paul, S. Kalita, S. Kalita, P. Sukumar and B. Mandal, *Sci. Rep.*, 2017, **7**, 1–13.
24 A. Sharma, P. Tiwari and A. Dutt Konar, *J. Mol. Struct.*, 2018, **1161**, 44–54.
25 D. Dev, N. B. Palakurthy, K. Thalluri, J. Chandra and B. Mandal, *J. Org. Chem.*, 2014, **79**, 5420–5431.
26 R. S. Giri, S. R. Manne, G. Dolai, A. Paul, T. Kalita and B. Mandal, *ACS Omega*, 2017, **2**, 6586–6597.
27 J. S. Richardson, *Adv. Protein Chem.*, 1981, **34**, 167–339.
28 E. G. Hutchinson and J. M. Thornton, *Protein Sci.*, 1994, **3**, 2207–2216.

29 A. Dutt, R. Frohlich and A. Pramanik, *Org. Biomol. Chem.*, 2005, **3**, 661–665.
30 R. Bosch, G. Jung, K. P. Voges and W. Winter, *Liebigs Ann. Chem.*, 1984, 1117–1128.
31 G. Jung, H. Bruckner, R. Bosch, W. Winter, H. Schaal and J. Strale, *Liebigs Ann. Chem.*, 1983, 1608–1622.
32 A. D. Konar, *CrystEngComm*, 2013, **15**, 10569–10578.
33 M. A. Spackman and D. Jayatilaka, *CrystEngComm*, 2009, **11**, 19–32.
34 M. A. Spackman and J. J. McKinnon, *CrystEngComm*, 2002, **4**, 378–392.
35 R. S. Giri and B. Mandal, *CrystEngComm*, 2018, **20**, 4441–4448.
36 *CrysAlisPro Oxford Diffraction Ltd. version 1*, 2009, 171. 33.34d.
37 G. M. Sheldrick, *Acta Crystallogr., Sect. A: Found. Crystallogr.*, 2008, **64**, 112–122.
38 S. K. Wolff, D. J. Grimwood, J. J. McKinnon, M. J. Turner, D. Jayatilaka and M. A. Spackman, *CrystalExplorer 3.1*, University of Western Australia, 2012.